

A Novel Fiber-Optic Interface for Unenhanced External Reflection Raman Spectroscopy of Supported Monolayers

Chad L. Leverette and Richard A. Dluhy*

University of Georgia, Department of Chemistry, Athens, Georgia 30602-2556

Received October 13, 1999. In Final Form: January 24, 2000

A novel sample interface has been developed to acquire the unenhanced external reflection Raman spectra of Langmuir–Blodgett thin films deposited onto solid substrates. This interface does not rely on a surface or resonance enhancement to amplify the monolayer signal, but rather uses fiber optics and gradient-index lenses for collection of the scattered light, thus providing an efficient collection mechanism for the Raman scattered radiation in an external reflection arrangement. This design is relatively inexpensive and straightforward to implement, resulting in a sensitive and fast tool for obtaining high-quality Raman spectra of ultrathin films (≥ 2.5 nm thickness). The results of this study show that a fiber-optic bundle provides an efficient mechanism for transfer of the scattered Raman radiation from the sample to the monochromator. The optical design also incorporates gradient-index lenses for image transfer onto the fiber bundle, thereby significantly reducing chromatic and spherical aberrations in the transfer of the image of the sample onto the fiber. Using this optical design, the spectrum of a single cadmium arachidate (Cd:Ar) monolayer transferred onto CaF_2 results in a signal-to-noise ratio of $\sim 400:1$ in the $\nu(\text{C}-\text{H})$ stretching region. Additionally, a high reflectivity dielectric mirror can be used as an alternative substrate to acquire Raman spectra below 2000 cm^{-1} . By use of this dielectric substrate, the unenhanced external reflection Raman spectrum of a Cd:Ar monolayer in the $\nu(\text{C}-\text{C})$ spectral region was obtained for the first time.

Introduction

Monomolecular films have received a great deal of attention in materials science, in part due to a rapid development of surface-sensitive characterization techniques, which enable investigation of the structural properties of these samples on the molecular level. In particular, Langmuir–Blodgett (L–B) films have become attractive model systems for determining the relationship between thin film structure and function.^{1,2} As the understanding of surface chemistry of monolayer films has evolved over the past 2 decades, more sensitive analytical methods have been developed to obtain spectra of these thin films with reasonable signal-to-noise (S/N) ratios. For L–B films transferred to solid substrates, some of the most sensitive characterization methods include diffraction^{3,4} and fluorescent techniques.^{5,6}

In addition to diffraction and imaging techniques, advances in instrumentation and methodology have enabled vibrational spectroscopy (i.e., IR and Raman spectroscopies) to become true surface-sensitive analytical methods for thin films and monolayers.^{7–10} Both of these

vibrational techniques provide direct information on the nature, conformation, and organization of complex molecular systems. Due to its ease of experimental design, as well as simpler instrumental requirements, IR spectroscopy has been the more widely applied vibrational method to surfaces and interfaces.⁹ For Raman spectroscopy, some type of enhancement of the weakly scattered light through surface (surface-enhanced Raman spectroscopy, SERS) or resonance enhancement (resonance Raman spectroscopy, RRS), or through the use of waveguides (Waveguide Raman Spectroscopy, WRS), has generally been required to amplify the very weak Raman scattering from thin films.^{9,11} Although these enhanced Raman methods are excellent tools for the study of surfaces and interfaces, each has its own drawbacks relating to interpretation, mechanism, or complexity that limits its routine use for most samples.¹¹

Although not as widely applied to the study of thin films, unenhanced Raman spectroscopy is equally as powerful as IR for studying L–B films due to its sensitivity to internal molecular structure, the chemical nature of the molecule, and the local molecular environment. Unenhanced Raman spectroscopy gives several advantages over IR for characterization of hydrocarbon assemblies, namely, sensitivity to chain backbone as well as intra- and intermolecular lateral interactions, in addition to having the ability to detect low-frequency vibrational modes.^{12–15}

It should therefore be possible, in principle, to use unenhanced Raman scattering as well as IR absorption

* To whom correspondence should be addressed. Phone, (706) 542-1950. Fax: (706) 542-9454. E-mail, dluhy@sunchem.chem.uga.edu.

(1) Kuhn, H.; Möbius, D.; Bucher, N. In *Physical Methods in Chemistry*; Weissberger, A., Rossiter, B. W., Eds.; Wiley-Interscience: New York, 1972; Vol. I, Part 3B, p 577.

(2) Roberts, G. G. *Adv. Phys.* **1985**, *34*, 475.

(3) Helm, C. A.; Möhwald, H.; Kjaer, K.; Als-Nielsen, J. *Biophys. J.* **1987**, *52*, 381.

(4) Jacquemain, D.; Grayer-Wold, S.; Leveiller, F.; Deutsch, M.; Kjaer, K.; Als-Nielsen, J.; Lahav, M.; Leiserowitz, L. *Angew. Chem., Int. Ed. Engl.* **1992**, *31*, 130.

(5) McConnell, H. M. *Annu. Rev. Phys. Chem.* **1991**, *42*, 171.

(6) Knobler, C. M.; Desai, R. C. *Annu. Rev. Phys. Chem.* **1992**, *43*, 207.

(7) Rabolt, J. F.; Swalen, J. D. In *Spectroscopy of Surfaces*; Clark, R. J. H., Hester, R. E., Eds.; John Wiley & Sons: London, 1988; Vol. 16, p 1.

(8) Mendelsohn, R.; Brauner, J. W.; Gericke, A. *Annu. Rev. Phys. Chem.* **1995**, *46*, 305.

(9) Dluhy, R. A.; Stephens, S. M.; Widayati, S.; Williams, A. D. *Spectrochim. Acta* **1995**, *51A*, 1413.

(10) Dluhy, R. A. In *Physical Chemistry of Biological Interfaces*; Baszkin, A., Norde, W., Eds.; Marcel Dekker: New York, 1999; p 711.

(11) Suëtaka, W. *Surface Infrared and Raman Spectroscopy*; Plenum Press: New York, 1995.

(12) Snyder, R. G.; Hsu, S. L.; Krimm, S. *Spectrochim. Acta* **1978**, *34A*, 395.

(13) Snyder, R. G.; Scherer, J. R. *J. Chem. Phys.* **1979**, *71*, 3221.

(14) Snyder, R. G.; Strauss, H. L.; Elliger, C. A. *J. Phys. Chem.* **1982**, *86*, 5145.

(15) Levin, I. W. In *Advances in Infrared and Raman Spectroscopy*; Clark, R. J. H., Hester, R. E., Eds.; Heyden-Wiley: Chichester, 1984; Vol. 11, p 1.

spectroscopy to provide complementary vibrational spectroscopic information into the structure of thin films. However, because of the different excitation mechanisms inherent in Raman and IR, and the decrease in Raman scattering volume when working with thin film samples, it has been difficult to acquire unenhanced Raman studies of monolayer films. This is shown by the fact that only a few research groups have published Raman spectra of supported monolayer and multilayer films.^{16–20}

The first report of unenhanced Raman spectroscopy to study thin films used a charge-coupled-device (CCD) detector to acquire a spectrum of a monolayer of cadmium stearate on a silicon substrate using 360-s integrations and achieving a signal-to-noise (S/N) ratio of $\sim 15:1$.¹⁶ In this work, the authors relied on binning of the CCD chip, as well as correcting each image for contributions due to the noise to acquire the thin film Raman spectra. Okamura et al.¹⁸ reported the use of unenhanced total reflection Raman spectroscopy to analyze the surface-pressure dependence of the structure in lipid L–B films. This group also focused on the $\nu(\text{C–H})$ stretching region to monitor lateral and conformational changes of the acyl groups of the lipid as a function of increasing surface pressure. To obtain the sensitivity needed to gather information about structural changes in the monolayers, all transfers were prepared with at least nine monolayers of lipid deposited onto a quartz prism. Thompson and Pemberton reported on the use of unenhanced Raman spectroscopy for characterization of alkylsilane and stearic acid multilayers on Al_2O_3 .¹⁹ This group also obtained information on the alkyl chain conformation of the thin films by monitoring the changes in the $\nu(\text{C–H})$ spectral region of these films as well as a spectrum of the $\nu(\text{C–C})$ region for octadecylsilane. A more recent study by Castaings et al.²⁰ reported on the use of a confocal Raman microscope to study cadmium arachidate (Cd:Ar) monomolecular films deposited onto CaF_2 . Spectra of the $\nu(\text{C–H})$ region and the $\nu(\text{C–D})$ region of hydrogenated and deuterated Cd:Ar multilayer and monolayer thin films were reported with good S/N ratios.

As seen from this discussion, unenhanced Raman spectroscopy is an underutilized technique for the study of thin films due to the difficulty inherent in acquiring weak photon scattering from surfaces. To enable unenhanced Raman spectroscopy to become more routinely useful for the study of thin films, spectra with higher S/N ratios must be obtained so that these spectra can be used to determine molecular structure. Also, optical designs must be efficient and robust, enabling routine collection of thin film spectra. In this current work, we introduce a novel sample interface using fiber optics to acquire the unenhanced external reflection Raman spectra of supported monolayer films. The optical design described here is straightforward to implement, thereby enabling routine collection of unenhanced, external reflection Raman spectra of transferred thin films. The fiber-optic interface enables the sample to be some distance away from the spectrometer without sacrificing the quality of the spectra. For comparison with previous work in this area, the model system chosen for study is cadmium arachidate (Cd:Ar) monolayers deposited onto two different dielectric sub-

strates. Using the optical interface described here, we have been able to obtain a signal-to-noise ratio of $\sim 400:1$ for the asymmetric $\nu(\text{C–H})$ stretching mode in a single Cd:Ar monolayer deposited onto a CaF_2 crystal. This design gives high-quality Raman spectra of both the high- and low-frequency vibrational modes of supported monomolecular films.

Materials and Methods

Surface Chemistry. Arachidic acid (Matreya, Inc., Pleasant Gap, PA) was dissolved in chloroform at a final concentration of 1 mg/mL. Monomolecular films of arachidic acid were formed by spreading the arachidic acid CHCl_3 stock solution onto the air–water (A/W) interface of a Langmuir–Blodgett (L–B) films balance (Joyce-Loebl, Ltd., Gateshead, England). The surface film was then allowed to equilibrate for 10 min before film compression was begun. The L–B trough subphase consisted of a 0.25 mM CdCl_2 solution, made using 18.2 M Ω /cm water from a Barnstead Nanopure system, and was thermostated to 22 °C. L–B depositions were performed at a surface pressure of 30 mN/m.

Substrates for Monolayer Film Deposition. Cadmium arachidate monolayers were transferred onto two separate substrates for spectroscopic analysis. The first substrate consisted of CaF_2 disks (25 mm \times 2 mm, Spectral Systems, Hopewell Junction, NY). CaF_2 has previously been used as substrates for Raman spectroscopic analysis of thin films (see, e.g., refs 16 and 20). The CaF_2 substrate was very effective in studying thin films in the C–H stretching region (between 2800 and 3000 cm^{-1}). Unfortunately, due to a large fluorescence background caused by visible wavelength excitation of trace impurities in the CaF_2 crystal, spectral regions lower than 2000 cm^{-1} could not be observed.

High reflectivity laser-line dielectric mirrors (25 mm \times 6 mm, Newport Corp., Irvine, CA) were the second type of substrate used for monolayer transfers. These high reflectivity mirrors are nonmetallic and have a reflective surface that is a composition of TiO_2 and SiO_2 multilayers. Since these mirror surfaces do not have the presence of any metal ions, particularly Ag or Al, no resonance enhancement of the Raman scattering takes place. These mirrors were used as a substrate because they effectively reflect the visible laser excitation, their thermal expansion is nominally zero (unlike other opaque substrates, i.e., Ge and Si), and they exhibit a low, noninterfering background at low wavenumber shifts (i.e., $<2000 \text{ cm}^{-1}$).

Langmuir–Blodgett Films of Fatty Acids. Langmuir–Blodgett films of fatty acid salts were deposited onto substrates for spectroscopic characterization using a Joyce-Loebl (Gateshead, England) Langmuir–Blodgett trough. The substrate was immersed in the subphase, after which the arachidic acid in CHCl_3 solution was spread on the water surface. After the equilibration period, the monolayer was compressed to the desired final surface pressure of 30 mN m^{-1} at a rate of 0.5 $\text{cm}^2 \text{ min}^{-1}$. The substrate was then vertically raised through the compressed monolayer film at a rate of 20 mm min^{-1} while the surface pressure was held constant (estimated deviation from the set pressure, $<\pm 1 \text{ mN m}^{-1}$), and the monolayers were deposited in a single pass through the interface. This process was repeated as needed for the buildup of multilayer films. Deposition of a single monolayer in each pass was assured by monitoring the transfer ratio for each substrate.

Raman Spectroscopy. Raman spectra were obtained on a ISA 500M #4 0.5-m single spectrometer equipped with a Spectrum One CCD2000 charge-couple device detector (Instruments SA, Edison, NJ). The CCD chip (SiTe ST-005A) is 2000 \times 800 pixels in size, back illuminated, with an individual pixel size of 15 μm . The detector is liquid nitrogen cooled to a temperature of $-140 \text{ }^\circ\text{C}$ and is back thinned giving a quantum efficiency of 85% at 550 nm. The grating used in the spectrometer had 1200 grooves/mm with a blaze wavelength of 750 nm; the slit width used in these experiments was typically 0.30 mm. For thin films deposited on CaF_2 , the Raman spectra were collected with 60-s integration times. An integration time of 240 s was used to acquire the Raman spectra of thin films deposited on the high reflectivity mirrors.

(16) Dierker, S. B.; Murray, C. A.; Legrange, J. D.; Schlotter, N. *Chem. Phys. Lett.* **1987**, *137*, 453.

(17) Kawai, T.; Umemura, J.; Takenaka, T. *Chem. Phys. Lett.* **1989**, *162*, 243.

(18) Okamura, E.; Umemura, J.; Takenaka, T. *J. Raman Spectrosc.* **1991**, *22*, 759.

(19) Thompson, W. R.; Pemberton, J. E. *Langmuir* **1995**, *11*, 1720.

(20) Castaings, N.; Blaudez, D.; Desbat, B.; Turlot, J.-M. *Thin Solid Films* **1996**, *284–285*, 631.

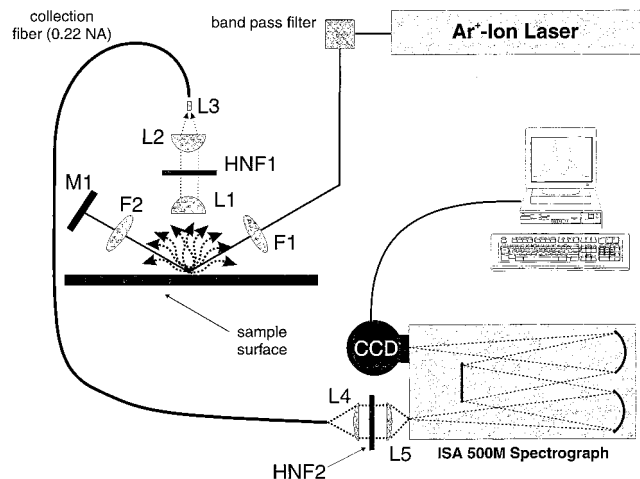


Figure 1. Schematic diagram of the fiber-optic interface used for unenhanced external reflection Raman spectroscopy of supported thin films. 514.5-nm laser radiation from a Coherent 305 Ar⁺-ion laser is directed through a holographic band-pass filter (Kaiser Optical Systems, HLBF-514) and steered onto the sample using a pair of *f*/2 plano-convex lenses (F1 and F2, Newport Optics, KPX082AR.14) to focus the collimated laser beam to a spot on the sample. M1 is a high-reflectivity 514.5-nm dielectric mirror (Newport Optics, 10Z20DM.5) used to redirect the reflected laser beam back onto the sample, thus increasing the local laser power density. The design of the scattered light collection optics (L1, L2, HNF1, and L3) is described in more detail in Figure 2. L4 is a *f*/2.2 achromatic doublet (Melles Griot, 01 LAO 037) and L5 is a *f*/4 achromatic doublet (Melles Griot, 01 LAO 135); the combination of L4 and L5 is used to *f*#-match the output of the fiber optic bundle (NA = 0.22) to the monochromator (NA = 0.125). HNF2 is a 514.5-nm holographic notch filter (Kaiser Optical HSPF-514) that eliminates any residual Rayleigh scattering from entering the monochromator.

A schematic illustration of the Raman spectroscopic setup is shown in Figure 1. A Coherent Radiation Innova 300 Series Ar⁺ laser (Coherent, Santa Clara, CA) provided the excitation radiation at 514.5 nm. The laser radiation was filtered using a wavelength-specific, 514.5 nm holographic band-pass filter (Kaiser Optical Systems, Ann Arbor, MI) to ensure beam quality and was steered with mirrors to the sample interface. Typical laser power at the sample was ~1.5–2 W. The beam was focused onto the sample with a plano-convex lens at an angle 60° to the surface normal resulting in a focused spot approximately 30 μm in diameter. One unique aspect of our sampling geometry is that the laser radiation reflected from the sample was collected by a plano-convex lens, recollimated and rereflected off a mirror that directed the laser radiation back through the same focusing lens and onto the sample for a second time (Figure 1). The second spot generated from the back reflection was overlaid with the incoming radiation spot to achieve greater power density at the sample location. With this optical arrangement, the typical power density at the sample is calculated to be ~3 × 10⁵ W cm⁻². This P_D is approximately an order of magnitude less than that encountered when using confocal Raman microscopes that have been used in studies of transferred monolayers on CaF₂.²⁰ With this current optical arrangement and P_D , we have not observed any degradation of the monolayer film over time.

The optical design for the collection of the Raman scattered radiation was optimized using an optical ray trace program (ZEMAX, Focus Software, Tucson, AZ). The details of the collection geometry for the Raman scattered radiation are shown in Figure 2. Figure 2A illustrates a ray trace through the optical interface for both paraxial as well as marginal rays. The current optical configuration has a field of view that allows objects with heights no greater than 3 mm to be imaged effectively onto the GRIN lens. This is illustrated in Figure 2A for object spots ±1.5 mm away from the optical axis. In this optical ray trace, the Raman scattering from the surface normal is collected by the surface of least radius of curvature of a *f*/2 achromatic doublet

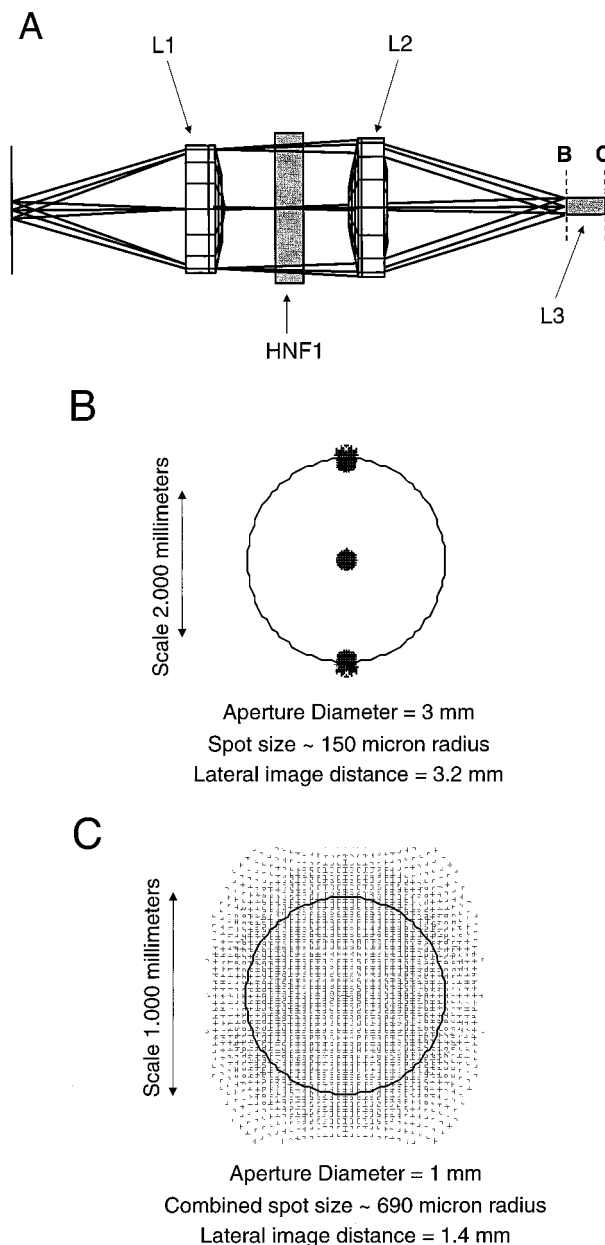


Figure 2. (A) Optical ray tracing diagram for the optimized *f*/2 optical configuration used to collect the external reflection scattered radiation from the sample surface. L1 is a *f*/2 achromatic doublet lens fabricated from BK7 glass (Newport Optics, PAC040) used to collect and collimate the scattered radiation. HNF1 is a 514.5-nm holographic notch filter (Kaiser Optical Systems, HSPF-514) inserted into the collimated beam to prevent Rayleigh scattered radiation from entering the collection fiber-optic bundle. L2 is a *f*/2 GRADUUM gradient-index achromatic doublet lens (Newport Optics, GAC040) that focuses the collimated light onto the front surface of a 0.25-pitch, plano-plano GRIN lens (SELFOC, NSG, Inc.). Positions "B" and "C" represent the front and back surfaces, respectively, of the GRIN lens. The GRIN lens is directly coupled to the surface of the fiber-optic bundle at position "C". This figure illustrates the ray trace for both paraxial and marginal rays of on-axis and off-axis focused points. (B) Optical ray footprint diagram of the object spots in image space focused onto the front surface of the GRIN lens at position "B", shown in Figure 2A. (C) Optical ray footprint diagram of the back surface of the GRIN lens at position "C", shown in Figure 2A, which is also the front surface of the fiber-optic bundle. The scale of the footprint diagram (1 mm) represents the diameter of the fiber-optic bundle surface.

lens (L1 in Figure 2A) (Newport Optics, Irvine, CA). The collimated radiation exiting this achromatic doublet *f*/2 lens

passes through a 514.5 nm holographic notch filter (HFN1 in Figure 2A) (Kaiser Optical Systems, Ann Arbor, MI) to remove most of the Rayleigh scattering prior to the radiation entering the collection fiber-optic bundle. The placement of the 514.5 nm notch filter at this position is crucial to prevent the intense Rayleigh scattering from exciting the silica vibrations of the collection fiber optic bundle, thus generating unwanted Raman silica background.

After the holographic notch filter, the collimated radiation is directed into a second $f/2$ achromatic doublet lens that focuses the collimated radiation (L2 in Figure 2A). In the present design shown in Figure 2A, the two $f/2$ optics give a magnification of unity for the sample radiation spot in image space. However, optical aberrations are always present in lens design and affect the quality of the resulting image. In the present case, the two main aberrations were calculated to be spherical and chromatic. To reduce these aberrations, the second $f/2$ lens (L2) was replaced with a $f/2$ achromatic doublet gradient-index lens (GRADIUM, Newport Optics) in which the refractive index of the optical glass varies axially along the optical axis. For gradient-index lenses, the greater the variations in lens refractive index, the greater the correction for the spherical and chromatic aberrations. The GRADIUM $f/2$ lens used in this study was chosen for its ability to significantly reduce both spherical and chromatic aberrations in the current design.

The GRADIUM $f/2$ lens focused the scattered radiation onto the front surface of a 0.25-pitch plano-plano, 3 mm diameter GRIN lens (position "B", Figure 2A) (SELFOC, NSG, Japan). Figure 2B illustrates an optical ray footprint diagram at the GRIN lens surface that demonstrates the location of the three focused object spots diagrammed in Figure 2A. These spots correspond to on-axis and off-axis focus points within the field of view of the interface. The optical ray footprint diagram shown in Figure 2B shows the diameter of the GRIN lens. Figure 2B demonstrates that although the magnification of this optical design is unity, the image spots on the limit of the field of view still contain some out-of-focus rays due to residual optical aberrations. Therefore, for optimal performance, alignment of the scatterer under the interface must be within ± 1.5 mm from the optical axis. This will allow for the image of the sample spot to be effectively transferred through the interface to the front surface of the GRIN lens with minimal aberration.

Figure 2C illustrates an optical ray footprint diagram for the light at the back surface of the GRIN lens (position "C", Figure 2A). The scale of the footprint diagram in Figure 2C (1 mm) represents the diameter of the fiber optic bundle used to transfer the scattered radiation to the monochromator. As seen in Figure 2C, the function of the GRIN lens is to transform the image spots on the front surface of the GRIN into a combined uniform spot that is then transferred into the fiber optic bundle. This 0.25-pitch GRIN lens transforms the three image spots separated by 3.2 mm shown in Figure 2B into a uniform spot with a diameter of 1.4 mm.

The back surface of the GRIN lens couples the light directly into a 12 around 6 around 1 fiber optic bundle. Each fiber in this bundle has a 200- μm core diameter and a 0.22 NA (Fiberguide Industries, Inc., Stirling, NJ). The spectrometer end of the fiber bundle was arranged in a 1×19 parallel line. The fiber optic bundle was brought to the spectrometer, and the output of the fiber parallel line was $f\#$ matched to the entrance slit of the spectrometer with a pair of achromatic doublet lenses (Figure 1). A second 514.5 nm holographic notch filter (Kaiser Optical Systems, Ann Arbor, MI) was placed between the $f\#$ -matching optics to eliminate the remainder of the Rayleigh scattered radiation from entering the monochromator.

All CCD spectral data were collected using the manufacturer-supplied SpectraMax for Windows software (Instruments SA, Edison, NJ). Postprocessing of the Raman spectra was performed using the Grams/32 software package (Galactic Industries, Nashua, NH). Wavelength calibration was performed using a 2nd order polynomial fit to Ne atomic emission lines²¹ using a Grams-based program written in our laboratory; wavenumber precision is estimated at better than ± 1 cm^{-1} . Any hard radiation

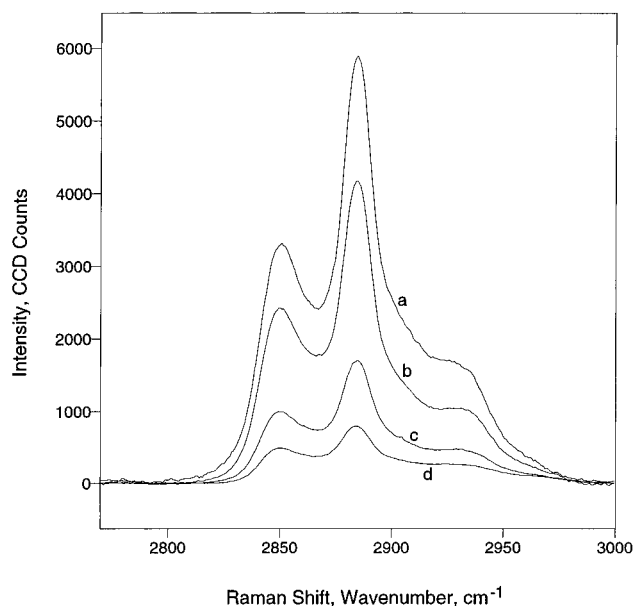


Figure 3. Unenhanced external reflection Raman spectra in the $\nu(\text{C-H})$ spectral region between 2750 and 3000 cm^{-1} of Cd:Ar Langmuir-Blodgett monolayers transferred onto CaF_2 disks. Curve a represents 21 monolayers, curve b represents 11 monolayers, curve c represents 5 monolayers, and curve d represents 1 monolayer

spikes present in the raw CCD Raman spectra were removed using a Grams-based CCD spike removal program written in our laboratory (R. Herrick and R. A. Dluhy, unpublished). This spike-correction program is based on previously published algorithms^{22,23} and provides a statistical approach using polynomial filters to identify and replace the spike-contaminated pixels. Unlike previously published methods,²² however, our current implementation of the spike-correction algorithm does not simultaneously smooth the spike-contaminated, raw CCD spectrum, thus preserving the original band shape. Baseline correction was performed on all spectra for clarity. Spectral subtraction of the background was performed only on the Raman spectra obtained from the dielectric mirror substrate. For the calculation of Raman band parameters and peak ratios, a Grams-based program was used to calculate the integrated intensities of the Raman spectral profiles. Other than spike removal, baseline correction, and spectral subtraction, the spectra presented in this paper have not been further processed in any way. In particular, the thin film Raman spectra presented in this paper have not been smoothed.

Results and Discussion

Using the optical interface presented schematically in Figures 1 and 2, unenhanced Raman spectra were obtained for supported multilayer and monolayer films of Cd:Ar. The $\nu(\text{C-H})$ stretching region (i.e., 2750–3000 cm^{-1}) in the Raman spectra of these transferred films is presented in Figures 3 and 4. In this wavenumber interval lies the spectral transitions characteristic of the methylene and methyl carbon-hydrogen (C-H) stretching vibrations.^{12–14} The three primary bands observed in our thin film Raman spectra were the 2850, 2880, and 2930 cm^{-1} modes, which correspond to the d^+ symmetric methylene $\nu_s(\text{C-H})$ stretching mode, the d^- asymmetric methylene $\nu_a(\text{C-H})$ stretching mode, and the multitude of overtones of the CH_2 bending modes, $\delta(\text{CH}_2)$, respectively. The band intensities and peak positions of the vibrations present in the Raman $\nu(\text{C-H})$ stretching region are a complicated function of both interchain lateral packing and intrachain

(21) Tseng, C.-H.; Ford, J. F.; Mann, C. K.; Vickers, T. J. *Appl. Spectrosc.* **1993**, *47*, 1808.

(22) Phillips, G. R.; Harris, J. M. *Anal. Chem.* **1990**, *62*, 2351.

(23) Hill, W.; Rogalla, D. *Anal. Chem.* **1992**, *64*, 2575.

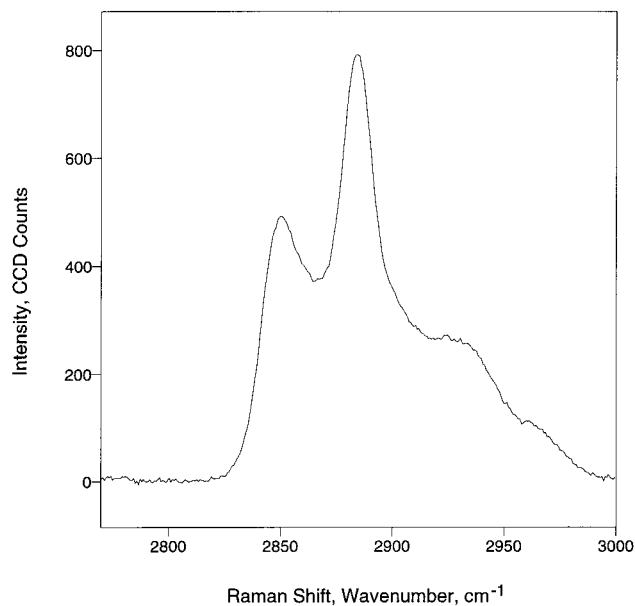


Figure 4. Unenhanced external reflection Raman spectrum in the $\nu(\text{C-H})$ spectral region of a single monolayer of Cd:Ar transferred to a CaF_2 disk. Acquisition parameters: 60-s integration times with 60 coadded spectra. S/N for the d^- asymmetric methylene vibration at 2880 cm^{-1} relative to the baseline is ca. 400:1.

conformational order in hydrocarbons.¹²⁻¹⁴ Although complicated, intensity ratios and band parameters derived from the Raman $\nu(\text{C-H})$ vibrational modes can be used to determine information about molecular structure in hydrocarbon and membrane assemblies.¹⁵

Figure 3 shows the Raman spectra for 21 (curve a), 11 (curve b), and 5 (curve c) multilayers and 1 (curve d) monolayer of cadmium arachidate transferred onto a CaF_2 substrate. The integrity of the Cd:Ar L-B transfers onto CaF_2 were monitored by calculating transfer ratios; in addition, the Raman scattering intensities were found to increase proportionally with the number of layers deposited. As seen in Figure 3, all of the unenhanced, external reflection thin film Raman spectra obtained with the current fiber optic interface have excellent signal-to-noise ratios. The frequency positions and the band shapes are the same for each of the different spectra regardless of the number of deposited layers, indicating a qualitatively similar chain structure for each of the transferred samples.

Figure 4 presents the Raman spectrum of a single monolayer of Cd:Ar on CaF_2 . For the monolayer spectrum in Figure 4 the S/N ratio was $\sim 400:1$ for the d^- asymmetric methylene $\nu(\text{C-H})$ stretching mode at 2880 cm^{-1} . This spectrum was acquired with 60-s integration times and 60 coadditions. In contrast, Figure 5 is a single monolayer spectrum with no coadditions. This spectrum represents raw data acquired in 60 s and has a S/N $> 70:1$ for the d^- asymmetric methylene $\nu(\text{C-H})$ stretching mode at 2880 cm^{-1} .

A Raman band parameter may be defined that compares the ratio between the integrated intensity areas of the 2880 cm^{-1} band and the 2850 cm^{-1} band. This ratio, $R_1 = I(\nu_a\text{CH}_2)/I(\nu_s\text{CH}_2)$, reflects both intermolecular lateral chain interactions as well as intramolecular (e.g., conformational) chain order¹⁶ and varies from 0.8 for totally disordered chains to 2.1 for a highly ordered crystal.²⁴ A relative decrease in the intensity of the d^- ($\nu_a\text{CH}_2$) with respect to the d^+ ($\nu_s\text{CH}_2$) is indicative of intramolecular

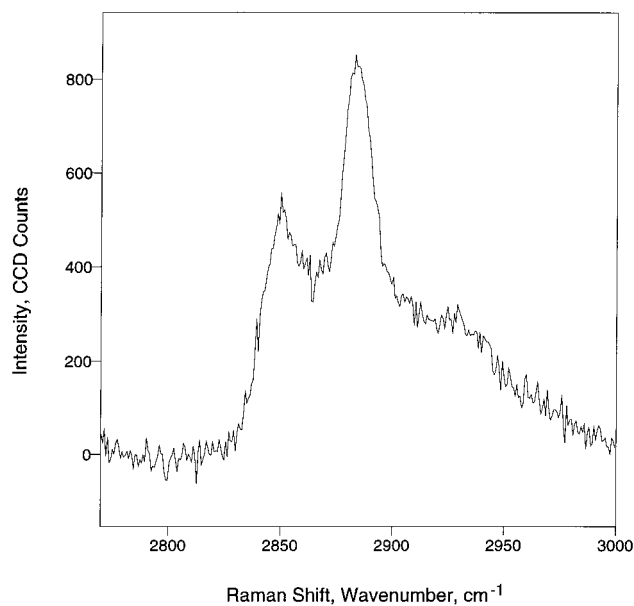


Figure 5. Unenhanced external reflection Raman spectrum in the $\nu(\text{C-H})$ spectral region of a single monolayer of Cd:Ar transferred to a CaF_2 disk. Acquisition parameters: 60-s integration time. S/N for the d^- asymmetric methylene vibration at 2880 cm^{-1} relative to the baseline is ca. 70:1.

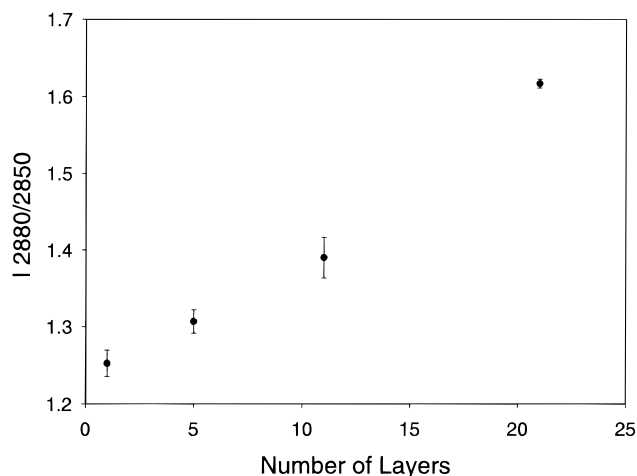


Figure 6. Variation of the Raman C-H intensity ratio parameter R_1 (i.e. I_{2880}/I_{2850}) with the number of monomolecular layers of Cd:Ar transferred onto CaF_2 substrates.

disordering of the monolayer.²⁰ Our values for R_1 for films transferred to CaF_2 are plotted versus number of transferred layers in Figure 6. The range of R_1 for L-B films transferred to CaF_2 varied from 1.2 for a single monolayer to 1.6 for 21 layers, thus showing that some additional conformational ordering or increased lateral interactions of the acyl chains occurred as the number of layers increased. For each of the samples studied here, three individual monolayer transfers were prepared, and the R_1 mean and standard deviation values for these samples are presented in Figure 6. Note that for each sample, the relative standard deviation is less than $\pm 2\%$.

A second Raman band parameter may be defined that more closely reflects the intramolecular chain ordering in hydrocarbon assemblies. It has been shown that the ratio between the integrated intensity areas of the 2930 cm^{-1} band and the 2880 cm^{-1} is a sensitive measure of intra-chain order/disorder processes in hydrocarbons.¹⁵ The ratio is calculated using the integrated intensity areas of the 2930 and 2880 cm^{-1} bands by $R_2 = I(\delta\text{CH}_2)/I(\nu\text{CH}_2)$.

(24) Bunow, M. R.; Levin, I. W. *Biochim. Biophys. Acta* **1977**, *487*, 388.

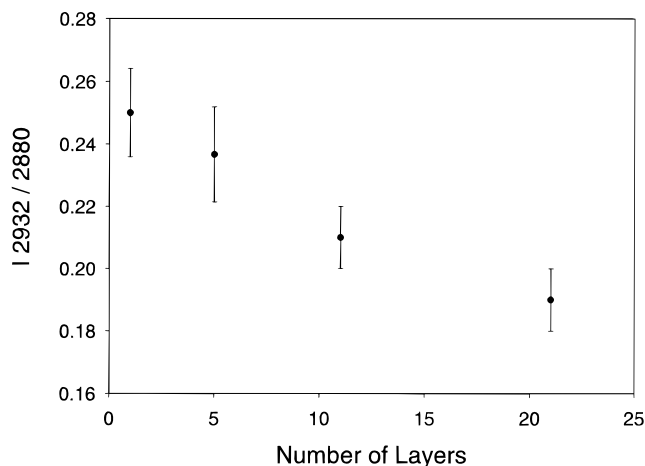


Figure 7. Variation of the Raman C–H intensity ratio parameter R_2 (i.e., I_{2930}/I_{2880}) with the number of monomolecular layers of Cd:Ar transferred onto CaF_2 substrates.

The R_2 parameter reflects increased intramolecular trans–gauche isomerization more than the R_1 parameter. For highly ordered lipid bilayers in the gel phase, the value of R_2 is ~ 0.4 .²⁴ Cadmium arachidate is known to be an even more highly ordered film than a lipid bilayer, since the cadmium ion helps to order the carboxylic acid headgroup of the fatty acid. The long acyl chain length of arachidic acid also helps to ensure a predominant all-trans configuration.

The values of R_2 for L–B films of Cd:Ar transferred to CaF_2 are plotted versus the number of transferred monolayers in Figure 7. The values of R_2 ranged from 0.26 for a single monolayer to 0.19 for 21 multilayers of Cd:Ar. The small overall decrease in the value of R_2 indicates a slight conformational ordering of the film with increasing numbers of L–B monolayers deposited to the substrate. As in Figure 6, the data plotted in Figure 7 were calculated as means and standard deviations from three independent samples for each number of layers. For R_2 , the relative standard deviation of each measurement is less than $\pm 6\%$. The larger value for the relative standard deviation of R_2 compared to R_1 is likely due to the difficulty associated with calculating an exact integrated intensities for the overtones of the CH_2 bending modes, $\delta(\text{CH}_2)$ at 2930 cm^{-1} .

These two Raman band parameters, R_1 and R_2 , give insight into intra- and intermolecular order and structure. The results show that, in general, the Cd:Ar thin films on CaF_2 substrates are very well ordered systems. However, as seen in Figures 6 and 7, a trend is evident that indicates a slight amount of increasing intermolecular and/or intramolecular conformational order as the number of transferred Cd:Ar monolayers increases.

In addition to CaF_2 , we used high-reflectivity dielectric mirrors as substrates for these external reflection Raman studies. The dielectric substrates were chosen in order to acquire unenhanced Raman spectra in the range below 2000 cm^{-1} , which is generally not possible using standard CaF_2 substrates due to intrinsic fluorescence in the CaF_2 material. Figure 8 illustrates a single monolayer spectrum of Cd:Ar acquired using the dielectric mirror as a substrate. This spectrum was acquired using 240-s integration times. The S/N ratio for this monolayer sample is comparable to that for the single monolayer on CaF_2 using a 60-s integration time (compare Figure 5 and Figure 8).

The difference in the integration times used for these two substrates is related to the optical properties of CaF_2 and the 60° incoming angle of incidence. By use of this

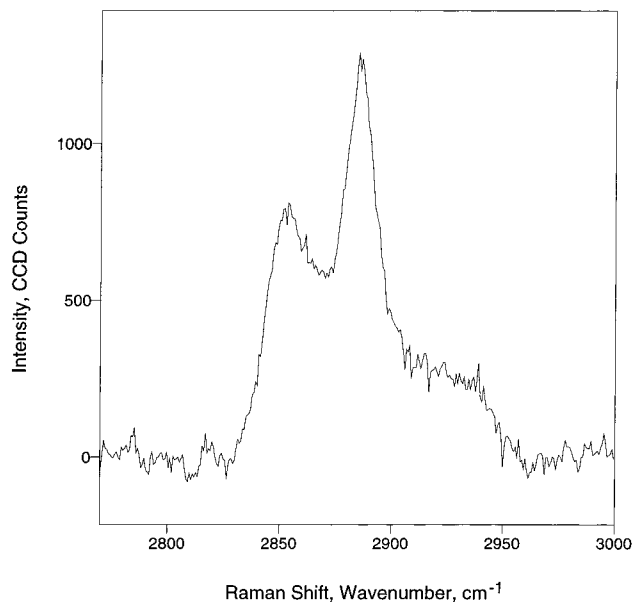


Figure 8. Unenhanced external reflection Raman spectrum in the $\nu(\text{C-H})$ stretching region of a single monolayer of Cd:Ar transferred to a high-reflectivity dielectric mirror.

experimental design, internal reflection will occur within the CaF_2 substrate, resulting in multiple scattering locations on the CaF_2 surface. For the conditions described here, several reflection points covered a lateral distance of approximately 3 mm on the CaF_2 surface, which is within the field of view of the $f/2$ collection lens, thus enabling all these scattering locations to be imaged onto the GRIN surface. This significantly increased the Raman scatter from the CaF_2 sample when compared to other substrates. For example, external reflection using the dielectric mirror substrate resulted in only one reflection location to be imaged; thus, longer integration times were necessary to collect the same scattering intensity as that obtained with the CaF_2 substrate.

The value of the intensity ratio R_1 for the Cd:Ar monolayer film transferred to the dielectric mirror shown in Figure 8 is 1.25. This value does not differ from the R_1 value calculated for a single Cd:Ar monolayer transferred to CaF_2 (1.25 ± 0.02 , Figure 6), thus indicating that the structure of the Cd:Ar monolayer is not changed by the choice of substrate. Similarly, the value of R_2 for a single Cd:Ar monolayer film transferred to the high reflectivity mirror was 0.26, a value that also falls within the range of R_2 values for a Cd:Ar monolayer transferred to CaF_2 (0.25 ± 0.01 , Figure 7). Again, a comparison of the value of R_2 for a single Cd:Ar monolayer on the two substrates showed that the molecular ordering of the film was the same on both substrates.

Further evidence of the presence of these highly ordered Cd:Ar monolayers comes from studying other regions of the spectrum. Figure 9 is a spectrum of the $\nu(\text{C-C})$ region for a Cd:Ar monolayer transferred to the high-reflectivity mirror. For comparison purposes, the $\nu(\text{C-C})$ region for bulk arachidic acid is plotted together with the Cd:Ar monolayer spectrum in Figure 9. The use of the high-reflectivity dielectric substrates allows us to acquire external reflection spectra in this region; Raman spectra could not be obtained for films transferred to CaF_2 due to strong fluorescence backgrounds in this region. For the Cd:Ar monolayer on the mirror, the $\nu(\text{C-C})_{\text{T}}$ ($\text{T} = \text{trans}$) bands at 1065 and 1127 cm^{-1} and the CH_2 trans twist mode at approximately 1297 cm^{-1} are clearly present. The presence of these bands and their strong intensities are

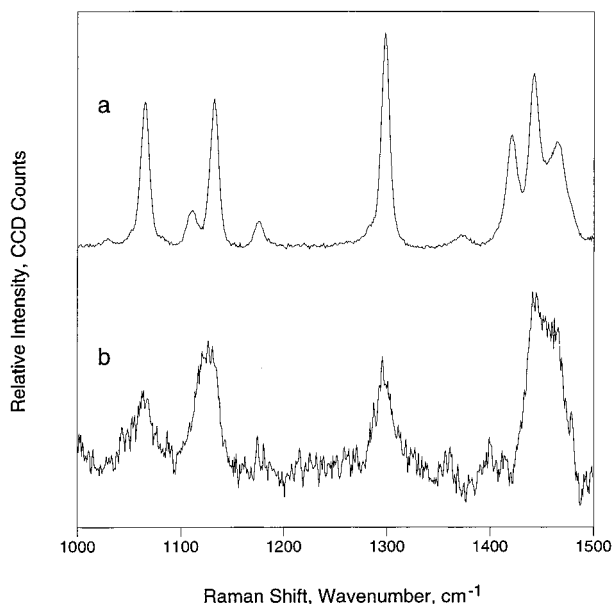


Figure 9. Raman spectra in the $\nu(\text{C}-\text{C})$ stretching region of Cd:Ar: (a) Raman spectrum of bulk arachidic acid; (b) unenhanced external reflection spectrum of a monolayer of Cd:Ar transferred to a high reflectivity dielectric mirror.

evidence of the highly all-trans order of this molecular monolayer transferred at high pressure. The absence of any band at approximately 1080 cm^{-1} which is due to the $\nu(\text{C}-\text{C})_{\text{G}}$ ($\text{G} = \text{gauche}$) is further evidence that the carbon backbone of the arachidic acid is predominantly in the all-trans configuration. The bands present around $1400\text{--}1500\text{ cm}^{-1}$ are due to the methylene deformation or bending modes. This spectrum represents the first time this valuable spectroscopic region of alkanolic acids has been reported without the use of any enhancement mechanisms.

Conclusions

We have developed a novel fiber-optic-coupled sample interface for the study of L-B thin films by unenhanced

external reflection Raman spectroscopy. This design is simple to construct, is relatively inexpensive to implement, and enables routine collection of the Raman spectra for thin film samples. The resulting spectra have excellent signal-to-noise characteristics for spectra obtained in a short amount of time with no resonance or surface enhancement of the sample. The main conclusions of this study are as follows:

A 19-fiber optic bundle consisting of $200\text{ }\mu\text{m}$ fibers arranged as a 12 around 6 around 1 bundle at the sample end and a 1×19 linear array at the spectrometer end provides an efficient mechanism for transfer of the scattered Raman light from a horizontal sample surface into the entrance slit of the monochromator.

A two-lens system consisting of dual $f/2$ lenses efficiently transfers the image of the sample onto the fiber bundle with unity magnification; however, significant chromatic and spherical aberrations can occur. These aberrations can be significantly reduced by using a second $f/2$ gradient-index lens that focuses the scattered radiation onto a plano-plano GRIN lens butt-coupled to the fiber-optic bundle.

Unenhanced external reflection Raman spectra of L-B transfers of Cd:Ar onto CaF_2 substrates acquired using this new sample interface results in high S/N spectra ($\sim 400:1$ for a single Cd:Ar monolayer). Analysis of the $\nu(\text{C}-\text{H})$ stretching region (i.e., $2750\text{--}3000\text{ cm}^{-1}$) reveals that these Cd:Ar films have an ordered molecular structure that agrees with previous Raman spectra of Cd:Ar fatty acid thin films.

A high-reflectivity dielectric mirror has been used as an alternative substrate to CaF_2 in the spectral regions below 2000 cm^{-1} . With this substrate, the unenhanced external reflection Raman spectra of a Cd:Ar monolayer in the $\nu(\text{C}-\text{C})$ spectral region was obtained for the first time.

Acknowledgment. The research presented here was supported by the U.S. Public Health Service through NIH Grant GM40117 (R.A.D.) and by the Thin Film Materials Science Initiative from the UGA Office of the Vice President for Research.

LA991347M